Autophagy 8:7, 1124–1135; July 2012; © 2012 Landes Bioscience

Loss of the starvation-induced gene Rack1 leads to glycogen deficiency and impaired autophagic responses in Drosophila

Balázs Érdi,[1†] Péter Nagy,[1†] Ágnes Zvara,[2] Ágnes Varga,[1] Karolina Pircs,[1] Dalma Ménesi,[2] László G. Puskás[2] and Gábor Juhász[1,*]

[1]Department of Anatomy, Cell and Developmental Biology; Eötvös Loránd University; Budapest, Hungary; [2]Laboratory of Functional Genomics; Biological Research Center; Tzeged, Hungary

[†]These authors contributed equally to this work.

Keywords: antimicrobial peptides, Atg8, autophagy, Drosophila, fat body, glycogen, GSK-3B, microarray, Rack1, starvation

Autophagy delivers cytoplasmic material for lysosomal degradation in eukaryotic cells. Starvation induces high levels of autophagy to promote survival in the lack of nutrients. We compared genome-wide transcriptional profiles of fed and starved control, autophagy-deficient *Atg7* and *Atg1* null mutant Drosophila larvae to search for novel regulators of autophagy. Genes involved in catabolic processes including autophagy were transcriptionally upregulated in all cases. We also detected repression of genes involved in DNA replication in autophagy mutants compared with control animals. The expression of *Rack1* (receptor of activated protein kinase C 1) increased 4.1- to 5.5-fold during nutrient deprivation in all three genotypes. The scaffold protein Rack1 plays a role in a wide range of processes including translation, cell adhesion and migration, cell survival and cancer. Loss of *Rack1* led to attenuated autophagic response to starvation, and glycogen stores were decreased 11.8-fold in *Rack1* mutant cells. Endogenous Rack1 partially colocalized with GFP-Atg8a and early autophagic structures on the ultrastructural level, suggesting its involvement in autophagosome formation. Endogenous Rack1 also showed a high degree of colocalization with glycogen particles in the larval fat body, and with Shaggy, the Drosophila homolog of glycogen synthase kinase 3B (GSK-3B). Our results, for the first time, demonstrated the fundamental role of Rack1 in autophagy and glycogen synthesis.

Introduction

The proper balance of anabolic and catabolic processes ensures cellular and organism-wide homeostasis under physiological conditions. Major intracellular catabolic pathways include the ubiquitin-proteasome system, responsible for the regulated degradation of selected proteins and autophagy, capable of degrading all intracellular macromolecules and even whole organelles. The major pathway of autophagy utilizes double-membrane vesicles called autophagosomes to deliver cytoplasmic cargo for degradation in lysosomes.[1] Basal levels of autophagy are required to prevent the accumulation of abnormal protein aggregates that are detrimental for cell function and survival, especially in long-lived cells such as neurons.[2-5] Autophagic activity is tightly controlled in all cells: factors increasing cell growth rate usually decrease, while nutrient or growth factor deprivation dramatically increases the levels of autophagy.[1]

A set of about 20 evolutionarily conserved genes required for autophagy has been identified in yeast. These *Atg* (autophagy-related) gene products orchestrate the formation of early autophagic structures where autophagosome generation takes place.[6] The Atg1 protein kinase complex is directly controlled by TOR (target of rapamycin), a kinase that coordinates growth-promoting stimuli with the availability of nutrients, ATP and oxygen. Inactivation of TOR rapidly activates the Atg1 complex, resulting in autophagy induction.[7] Autophagy also requires a specific phosphatidylinositol-3-kinase (PtdIns3K) complex, the transmembrane protein Atg9 and factors involved in its cycling from cellular reservoirs to phagophore assembly sites, and two ubiquitin-like protein conjugation systems that ensure lipidation and membrane association of the ubiquitin-like protein Atg8. Atg8 is associated with the surface of autophagosomes similar to a coat protein. Atg8 needs to be cleaved off from the outer membrane to allow the fusion of autophagosomes with lysosomes and endosomes, while the Atg8 pool associated with the inner membrane is degraded along with sequestered cargo in autolysosomes.[8,9] This way, half of these Atg8 protein molecules are broken down in each autophagosomal cycle.[10]

Yeast studies found that the levels of Atg8 can become rate-limiting during autophagy, and that upregulation of this gene is normally observed during induction.[1] In higher eukaryotes, increased transcription from *Atg8* homologs and other *Atg* genes has been documented in certain settings, for example in murine muscles, or in Drosophila fat body and salivary gland cells at the

*Correspondence to: Gábor Juhász; Email: szmrt@elte.hu
Submitted: 09/14/11; Revised: 03/19/12; Accepted: 03/19/12
http://dx.doi.org/10.4161/auto.20069

onset of metamorphosis, but not in all cases of autophagy induction.[11-15] Basal levels of Atg proteins and the extent of autophagy induction must together determine if transcriptional upregulation of these genes is necessary during the response. The presence of multiple homologs of a single yeast gene may also supply enough proteins to support autophagy induction. Interestingly, the *Atg8* gene family has expanded in higher eukaryotes, for example there are two members in Drosophila (*Atg8a* and *Atg8b*), and five in mammals with specialized functions during autophagosome formation (*GABARAP*, *GABARAPL1*, *GABARAPL2*, *GABARAPL3* and *MAP1LC3*—this latter gene also produces four different protein isoforms).[6,16]

Drosophila is an excellent model for autophagy studies, as polyploid tissues like the fat body grow rapidly during the larval stages, and store nutrients to support metamorphosis later on. Therefore, low levels of autophagy are observed during the feeding period in larval stages L1 (approximately 24–48 h after egg laying—AEL), L2 (48–72 h AEL) and most of L3 (72–120 h AEL). Larvae leave the food at around 108 h AEL (the onset of the wandering period) to find a proper, dry place for pupariation, which is observed around 120 h AEL. Robust induction of autophagy is seen in the larval fat body and midgut in wandering larvae, or in response to starvation during earlier stages.[17,18]

We have previously used transcription profiling to search for gene expression changes in dissected fat bodies of feeding and wandering animals. By following the expression levels of 3,200 genes, we found that Atg8 homologs were upregulated, and we have successfully shown that the downregulated gene *FKBP39* (FK506-binding protein of 39 kD) is an inhibitor of autophagy. FKBP39 likely acts by inhibiting the transcription factor Foxo, and we found for the first time that Foxo is an important positive regulator of autophagy.[15] Since then, Foxo-dependent transcriptional upregulation of *Atg8* homologs during autophagy has been described in murine muscles.[11,12]

We reasoned that a similar strategy could be applied by looking at gene expression changes during starvation. An earlier study reported a whole-genome analysis of starvation responses in 48 h AEL (L2 stage) larvae, and found the transcriptional induction of only *Atg8a* (annotated as *CG1534* at that time) and *Atg9* of all the autophagy genes.[19] We decided to use a more sensitive newer generation microarray platform to test 86 h AEL (L3 stage) larvae as these are used in most cases for studies on starvation-induced autophagy. In addition, this time point is after the developmental milestone known as the '70 h change.' This simply refers to the observation that all larvae before 70 h AEL die in a few days upon complete starvation, while a fraction of the larvae past 70 h AEL (near the L2- to L3-molt) that have presumably accumulated appropriate nutrient stores to sustain metamorphosis are able to pupariate and give rise to small adults.[20]

Results

Microarray analysis of starvation-induced autophagy in Drosophila larvae. We compared genome-wide expression changes of 86 h AEL control larvae subjected to a 4-h complete starvation to their well-fed siblings. We have also analyzed previously described autophagy-deficient null mutants for *Atg7* (on a similar genetic background with control larvae) and *Atg1* (from a distinct genetic background), with the purpose of finding gene networks that are specifically regulated in starved autophagy mutants.[3,21] Genes that showed at least a two-fold induction or repression with a p value < 0.05 were considered regulated. We found that the expression of 2,819 vs. 3,690 and 3,971 of 13,613 genes (represented by unique FBgn identifiers)[22] was starvation-regulated in controls, *Atg7* and *Atg1* mutants, respectively. Please see **Table S1** for detailed results.

Genes encoding antimicrobial peptides such as Drosomycin and IM10 (immune-induced molecule 10) were among the most highly upregulated genes in all three genotypes (**Table S2**). Growth/insulin signaling is inhibited in response to starvation, which activates the transcription factor Foxo (forkhead box, subgroup O).[15] Induction of these immune effector molecules is directly controlled by Foxo.[23] The FoxA/Forkhead transcription factor target gene *CG6770* which is transcriptionally induced upon inhibition of TOR was also induced 37- to 95-fold.[19,24] Another highly upregulated gene was *CG7224,* encoding a small, 118-amino acid protein. As it was transcriptionally induced 19.5- to 30.5-fold in the different genotypes, we named this gene *Sirup* (starvation-upregulated protein). Interestingly, expression of *Sirup* and its paralog *CG15283* was also induced during developmental autophagy of the fat body.[15]

Of the 20 genes showing the strongest downregulation, only two were found in all three genotypes: *CG15615* encoding an oxidoreductase (36- to 61-fold repression) and *CG15155* encoding a transferase that transfers acyl groups other than amino-acyl groups (30- to 60-fold repression; **Table S3**). The biological processes in which these gene products are involved are not known, and no phenotypic data are available for these genes.

We performed gene ontology (GO) analysis of the significantly regulated genes in the three different genotypes (**Fig. 1A and B**; **Tables S4 and S5** for details). The analysis revealed that genes belonging to 10 enriched GO categories were specifically induced in autophagy mutants (please see **Table S6** for a list of induced genes in these 10 Atg mutant-specific enriched GO categories). Some of these GO categories that are high in the hierarchy of GO terms (such as GO0009056: catabolic process) included genes that were also present in other, more specific GO groups enriched in all three genotypes, which is a clear limitation of GO analyses. Nevertheless, these groups include genes involved in the metabolism of purine nucleotides and in various catabolic processes, such as *CG9363* encoding an enzyme involved in the breakdown of tyrosine and L-phenylalanine. Numerous genes encoding members of the ubiquitin-dependent protein catabolic process were also found here, including *CHIP*, *CG1950*, *CG4661*, *CG18341* and *Ubc84D*.[22] Only 3 enriched GO terms were specific for autophagy mutants among repressed genes (please see **Table S7** for a list of repressed genes in these 3 Atg mutant-specific enriched GO categories). Genes in these categories encode proteins involved in DNA metabolism, amplification and replication, such as DNA polymerases CG8142, DNA polymerase α 73 kD and 180 kD, DNA polymerase delta, and essential DNA replication factors Mcm5

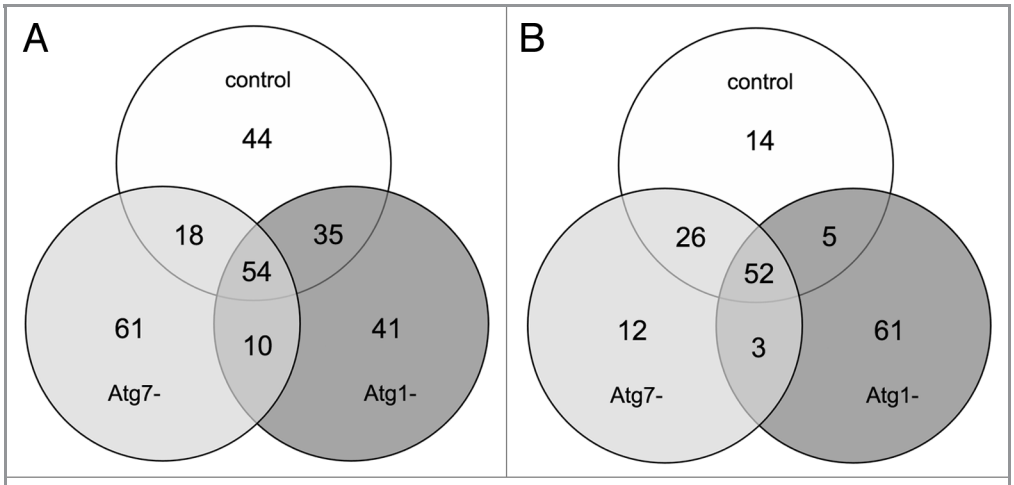

C

	control	Atg7	Atg1	Yeast Name	Drosophila Name	Drosophila CG number	Human Name	D QTPCR	
Atg1 complex	2	2.8	3.1	Atg1	Atg1	CG10967	ULK1	~~4.1~~	Atg1
	1.2	1.3	1.6	Atg13	Atg13	CG7331	Atg13	~~3~~	Atg13
	4.6	3	2.6	Atg17?	FIP200	CG1347	RB1CC1, FIP200	3.1	FIP200
	2.5	3.7	4.3	-	Atg101	CG7053	Atg101	2.2	Atg101
PI3P signaling	2.2	1.8	2.5	Atg6	Atg6	CG5429	Beclin1	~~5.2~~	Atg6
	1.2	1.3	1.6	Atg14	Atg14	CG11877	Atg14L, Barkor	~~4.6~~	Atg14
	1.8	2	1.9	Vps15	Vps15, ird1	CG9746	Vps15, p150	~~6~~	Vps15, ird1
	2	2.6	2.7	Vps34	Vps34, PI3K59F	CG5373	Vps34, PIK3C3	5.7	Vps34
	2.3	3.1	3.4	-	EDTP	CG6542	Jumpy, MTMR14	6.5	EDTP
Pre-autophagosomal cycling complex	2.8	3.4	3.3	Atg2	Atg2	CG1241	Atg2	24	Atg2
	3.7	5.5	4.9	Atg9	Atg9	CG3615	Atg9	15	Atg9
	3.2	4.3	4.5	Atg18	Atg18a	CG7986	WIPI2	11	Atg18a
	6.5	7.7	4.3	Atg18	Atg18b	CG8678	WIPI2	35	Atg18b
Ubiquitin-like conjugation systems	1.9	1.6	1.8	Atg3	Atg3, Aut-1	CG6877	Atg3	~~3.7~~	Atg3, Aut-1
	2.2	2.7	2.9	Atg4	Atg4a	CG4428	Atg4b	23	Atg4a
	0.7	0.7	0.9	Atg4	Atg4b	CG6194	Atg4d	8.4	Atg4b
	1.3	1.3	1.5	Atg5	Atg5	CG1643	Atg5	7.6	Atg5
	2.9	2.3	2.8	Atg7	Atg7	CG5489	Atg7	~~3.2~~	Atg7
	7.6	9.3	8.3	Atg8	Atg8a	CG32672	GABARAPL2	169	Atg8a
	2.3	3.8	2.2	Atg8	Atg8b	CG12334	GABARAPL1	118	Atg8b
	0.6	0.6	0.5	Atg10	Atg10	CG12821	Atg10	N/A	Atg10
	1.2	~~0.9~~	0.9	Atg12	Atg12	CG10861	Atg12	~~55~~	Atg12
	2.1	1.9	2.1	Atg16	Atg16	CG31033	Atg16	~~7.2~~	Atg16
Cargo selection	2.4	2.8	3.4	-	Blue cheese	CG14001	ALFY	10	Blue cheese
	5.1	6.6	6.2	-	Ref(2)P, p62	CG10360	p62, SQSTM1	4.8	Ref(2)P

0 10
fold change

Figure 1. Transcriptional analysis of starvation responses. The number of gene ontology (GO) terms enriched ($p < 0.05$) among the significantly upregulated (A) and downregulated (B) genes (minimum two-fold change in expression level during the 4-h complete starvation, $p < 0.05$) in control, *Atg7* and *Atg1* mutant larvae. See text and **Tables S4 and S5** for details. (C) lists starvation-induced transcriptional changes (gene expression levels in starved animals relative to the expression levels detected in fed animals) for Drosophila homologs of yeast and human *Atg* genes, involved in the core mechanism of autophagy. *Atg8a* encoding a ubiquitin-like protein showed the highest induction during starvation. Interestingly, the highest average upregulation was observed for genes encoding members of the Atg9 cycling complex. (D) Quantitative real-time (QT) PCR analysis of fat bodies dissected from fed and starved control larvae. Numbers represent fold change values, and nonsignificant changes are crossed out in (C and D).

(Minichromosome maintenance 5), Mcm10, disc proliferation abnormal, replication factor C subunits RfC3 and RfC38, double parked, DNA ligase I, SuUR (suppressor of under-replication), mus209/PCNA (proliferating cell nuclear antigen) and origin recognition complex subunit 2.[22]

Interestingly, we detected many more genes significantly regulated upon a 4-h complete starvation when compared with an earlier study.[19] Zinke et al. reported 369 and 279 genes significantly induced or repressed, respectively, while we found that 1,584 and 1,235 genes were significantly up- or down-regulated in control larvae, respectively. Comparing the list of hits revealed that 170 genes were found induced and 134 repressed in both studies (please see **Tables S8 and S9** for a list of these genes), which is almost half of all genes identified by Zinke et al. While some of these differences are likely due to the different genetic backgrounds and larval stages tested, we are convinced that our approximately 4.3-fold higher discovery rate is mostly due to the use of a different, more sensitive microarray. This is further supported by a previous study that compared different microarray technologies and found that the long oligonucleotide platform (such as in the case of our study utilizing arrays printed with 60-mer oligos) is more sensitive and produces lower levels of technical variability when compared with cDNA-based systems (used by Zinke et al.).[25]

Most autophagy genes are transcriptionally induced during starvation. Several GO terms that include *Atg* genes (such as GO0048102: autophagic cell death) were found enriched among the upregulated genes in all three genotypes. To focus more on autophagy, we looked at the expression of *Atg* gene homologs. Many of these genes showed increased induction in autophagy mutants compared with controls (**Fig. 1C**). Expression from the *Atg7* and *Atg1* loci was still observed in the mutants; since these alleles had been previously characterized as genetic nulls, presumably truncated versions of wild-type transcripts were detected.[3,21]

Of the genes encoding members of the Atg1 kinase complex, *Atg1*, *FIP200* and *Atg101* showed a moderate induction, while the levels of *Atg13* did not change. This is in agreement with recent findings that Atg13 is continuously degraded by the ubiquitin-proteasome system, and it is stabilized by the binding of Atg101 during autophagy induction.[26,27] Therefore, Atg13 protein levels appear to be mainly regulated on the post-translational level. It is important to note that *Atg101* showed the highest upregulation in this group (on average 3.5-fold in the 3 different genotypes), but it was mostly due to its stronger induction in autophagy mutants. In controls, *FIP200* shows the highest induction in this group (4.6-fold).

Genes encoding members of the autophagy-specific PtdIns3K complex (Vps34, Vps15, Atg6, Atg14) showed an even milder response: only *Vps34* that codes for the lipid kinase itself was upregulated in all three genotypes. To our surprise, *EDTP* (Egg-derived tyrosine phosphatase) showed the highest average induction in this lipid signaling group: 2.9-fold. This gene encodes the Drosophila homolog of the lipid phosphatase Jumpy, a potent antagonist of the autophagy-promoting activity of Vps34 in mammals.[28] The upregulation of a potential inhibitor of autophagy may represent a negative feedback loop that acts to prevent hyperactivation. Elucidation of this hypothetical mechanism needs further studies.

Interestingly, genes encoding members of the pre-autophagosomal cycling complex showed the strongest average induction, between 3.2- and 6.2-fold. Atg9 is the only transmembrane protein among *Atg* gene products, and it has been shown to cycle between early autophagic structures and potential intracellular membrane sources to ensure membrane transport to forming autophagosomes. Atg2 and Atg18 are required for the cycling of Atg9 in yeast.[29]

Half of the genes (5/10) encoding members of the ubiquitin-like protein conjugation systems did not even show an upregulation. *Atg4a*, *Atg7*, *Atg8b* and *Atg16* were moderately induced, while the highest upregulation of all the *Atg* genes was detected for *Atg8a*, 8.4-fold on average.

Atg8a itself is a specific cargo selectively degraded during autophagy. Additional substrates have also been described, such as p62/Ref(2)P, which is an intracellular receptor of ubiquitinated proteins for selective autophagy, in addition to its scaffolding roles in multiple signaling pathways. p62 binds to Atg8 homologs, so it is continuously degraded during autophagy.[30] We found that *p62* is transcriptionally induced 6-fold during starvation, potentially in part to compensate for its accelerated rate of degradation during increased autophagy. A more moderate upregulation was detected for *Blue cheese/Alfy*, whose protein product is involved in the selective degradation of cytosolic protein aggregates.[31]

Next we sought to expand on our findings obtained by microarray analysis of starved whole larvae by focusing on the fat body. We followed the expression of selected genes by quantitative real-time PCRs, comparing fat bodies dissected from starved vs. fed control larvae (**Fig. 1D**). These QT-PCR experiments further supported our most important findings: among the genes encoding members of the Atg1 kinase and lipid kinase complexes *EDTP* showed the highest upregulation (6.5-fold), which is still moderate when compared with genes that showed the strongest induction. *Atg8a* was by far the most highly upregulated gene (169-fold), and all members of the membrane transport group were strongly induced (11- to 35-fold). The expression of *Sirup* also increased 60.4-fold. There were also important differences, such as in the case of *Atg5* that showed a 7.6-fold upregulation in fat bodies while no significant change was detected in whole larvae, as it was probably masked by other tissues.

Rack1 is required for a full autophagic response to starvation. We selected a set of genes for further studies that were starvation-regulated in all three genotypes, and no autophagic function had been assigned to these in spite of having been already characterized to some extent. For example, *Rack1* transcription increased 4.1-, 5.5- and 4.1-fold in controls, *Atg7* and *Atg1* mutants, respectively. QT-PCR analysis also showed that *Rack1* was upregulated 21.6-fold in the fat body upon starvation.

Silencing of *Rack1* expression reduced autophagy based on mCherry-Atg8a (**Fig. 2A and N**), Lysotracker Red staining and Lamp-GFP, a reporter for lysosomes.[32] Numerous small, presumably inactive Lamp-GFP positive lysosomes were seen in

fat body cells of well-fed control larvae, which were not strongly acidic as revealed by lack of Lysotracker Red labeling (**Fig. 2B**). In contrast, large Lamp-GFP and Lysotracker-positive autolysosomes were formed during starvation (**Fig. 2C**). Silencing of *Rack1* reduced the number and size of Lysotracker and Lamp-GFP positive autolysosomes formed during starvation (**Fig. 2D**, see also **Fig. 2O–Q** for statistics).

To expand on these RNAi studies we have also analyzed a previously described null mutant *Rack1[1.8]*.[33] Using the same mCherry-Atg8a and Lysotracker assays, we observed again a strong reduction of autophagy in *Rack1* mutants compared with heterozygous controls (**Fig. 2E–H**; see also **Fig. 2N and O** for statistics). As a final proof for the role of Rack1 in autophagy, we have generated transgenic animals expressing Rack1 with a C-terminal FLAG-HA tag by using a DNA construct from the ongoing Drosophila proteomics project. Heat shock-mediated expression of Rack1 in mutant larvae partially rescued their autophagy defect (**Fig. 2I and O**). To avoid a possible effect of the heat shock on autophagy, all genotypes were heat shocked in these Lysotracker and electron microscopy experiments (see below).

Similar to the above findings, ultrastructural analysis showed that while numerous autophagosomes and large autolysosomes were observed in heterozygous controls, the cumulative area of these structures was decreased in cross-sections of *Rack1* mutant fat body cells, and heat shock-mediated expression of Rack1 in mutant larvae again showed a partial rescue (**Fig. 2J–M**; see **Fig. 2R** for statistics). The partial rescue effect may reflect insufficient expression levels, or more likely it may be caused by the C-terminal tag interfering with full protein activity. Still, the reduction of autophagosome area was completely rescued in these experiments ($p = 0.02$ for mutant and rescue, and $p = 0.84$ for control and rescue sample pairs, respectively), suggesting that Rack1 is required for efficient autophagosome formation (**Fig. 2L**).

Interestingly, we found that Rack1 was dispensable for developmental autophagy induced in fat body and midgut cells prior to metamorphosis in late L3 stage wandering animals (**Fig. S1C and S1D**). In contrast, p62 aggregates accumulated in Rack1 RNAi cells in well-fed early L3 stage animals (**Fig. S1E and S1F**). This finding suggests that Rack1 is also involved in basal autophagy, as the ubiquitin- and Atg8-binding protein p62 is continuously degraded by autophagy along with aggregated ubiquitinated proteins.[30]

Rack1 is involved in glycogen synthesis. Glycogen stores are normally present in fat body, midgut and muscle cells in Drosophila larvae. A striking phenotype of these *Rack1* mutant fat body cells was the 11.8-fold reduction of glycogen particle area compared with heterozygous controls in electron micrographs, and this effect was also partially rescued by Rack1 expression (**Fig. 2J–M**; see **Fig. 2S** for statistics). Reduced glycogen stores were most likely caused by defects in glycogen synthesis induced by the 4 h starvation in 20% sucrose rather than accelerated degradation, as no glycogen particles could be observed in fat bodies of well-fed control or *Rack1* mutant larvae (**Fig. S1A and S1B**). In these latter cases, the lack of glycogen was probably due to the high-protein diet that we routinely feed larvae before starving them, by supplementing the medium with live yeast paste. Taking advantage of a monoclonal antibody specific for glycogen, we were also able to show that silencing of *Rack1* decreased glycogen stores in a cell-autonomous manner in larvae fed a high sugar-high protein diet, that is, medium supplemented with live yeast paste prepared in 20% sugar; similar phenotypes were observed in mutants (**Fig. 2T–V**).

Endogenous Rack1 localizes to early autophagic structures and glycogen. Immunofluorescence analysis revealed that Rack1 is present in numerous cytoplasmic particles in most tissues. Knockdown of *Rack1* expression reduced staining both in fat body and midgut cells (**Fig. 3A and B**). To assess the potential role of Rack1 in autophagy, we performed colocalization experiments. Atg8a fusion proteins are the best characterized fluorescent reporters for autophagosome generation. We found that endogenous Rack1 colocalized with GFP-Atg8a in 5.8% of the cases (n = 10/171 dots) (**Fig. 3C**). Vice versa, 6.1% of GFP-Atg8a particles colocalized with Rack1 (n = 11/181 dots). In contrast, not a single case of colocalization was observed between endogenous Rack1 and the lysosome reporter Lamp1-GFP (**Fig. 3D**). We next used immunogold labeling of endogenous Rack1 to localize it on the ultrastructural level. We found that Rack1 was associated with 7.7% of pre-autophagosomal phagophores and autophagosomes (n = 17/221) (**Fig. 3E**; see also **Fig. 3G**). Again, no labeling of lysosomes was seen.

Figure 2 (See opposite page). Rack1 is required for the full autophagic response to starvation, and for efficient glycogen synthesis. (A) Knockdown of *Rack1* results in reduction of autophagy in response to starvation. Please compare the number of mCherry-positive dots in RNAi cells vs. control cells in each panel (red; the red channel is also shown in greyscale in insets). RNAi expressing cells are marked by coexpression of GFP (green). Cell nuclei are labeled with DAPI (blue). (B) Numerous small Lamp1-GFP dots are seen in fat body cells of well-fed control larvae, which are not co-labeled by Lysotracker Red. (C) In contrast, large Lamp1-GFP and Lysotracker-positive autolysosomes are formed during starvation. (D) Silencing of *Rack1* strongly reduces the number of Lysotracker particles that are formed during starvation; note that the size of Lamp1-GFP dots is also more similar to fed control cells. (E and F) The number of starvation-induced mCherry-Atg8a dots is reduced in *Rack1* null mutant fat bodies compared with controls. (G and H) Similarly, the number of Lysotracker-positive autolysosomes is reduced in *Rack1* mutants compared with controls. (I) Starvation-induced autophagy is rescued by heat shock-mediated expression of a *Rack1* transgene in *Rack1* null mutant animals. (J) Transmission electron microscopy shows the presence of large glycogen stores (g), numerous double-membrane autophagosomes (arrowheads) and autolysosomes (arrows) in fat body cells of control animals starved for 4 h in 20% sucrose. (K) A portion of (J) is shown enlarged. (L) Fewer autophagic structures and glycogen particles are detected in *Rack1* mutants. (M) Heat-shock mediated expression of a *Rack1* transgene in *Rack1* null mutant animals partially rescues the reduced autophagy and glycogen accumulation phenotypes of the mutants. (N–S) Statistical analyses of mutant and RNAi phenotypes on autophagy and glycogen stores. Graphs represent dots/cell (N–P), average dot size (Q) and normalized cytoplasmic area (R and S), $^{**}p < 0.01$ (two-tailed, two-sample unequal variance Student's t-test). (T) Knockdown of *Rack1* expression cell-autonomously decreases glycogen stores. (U and V) No specific Rack1 labeling is observed in *Rack1* mutants, and glycogen stores are strongly decreased compared with heterozygous controls. Scale bars: 30 μm for all fluorescent images (indicated in A, E and T–V), 10 μm for (J, L and M, indicated in J) and 2 μm for (K).

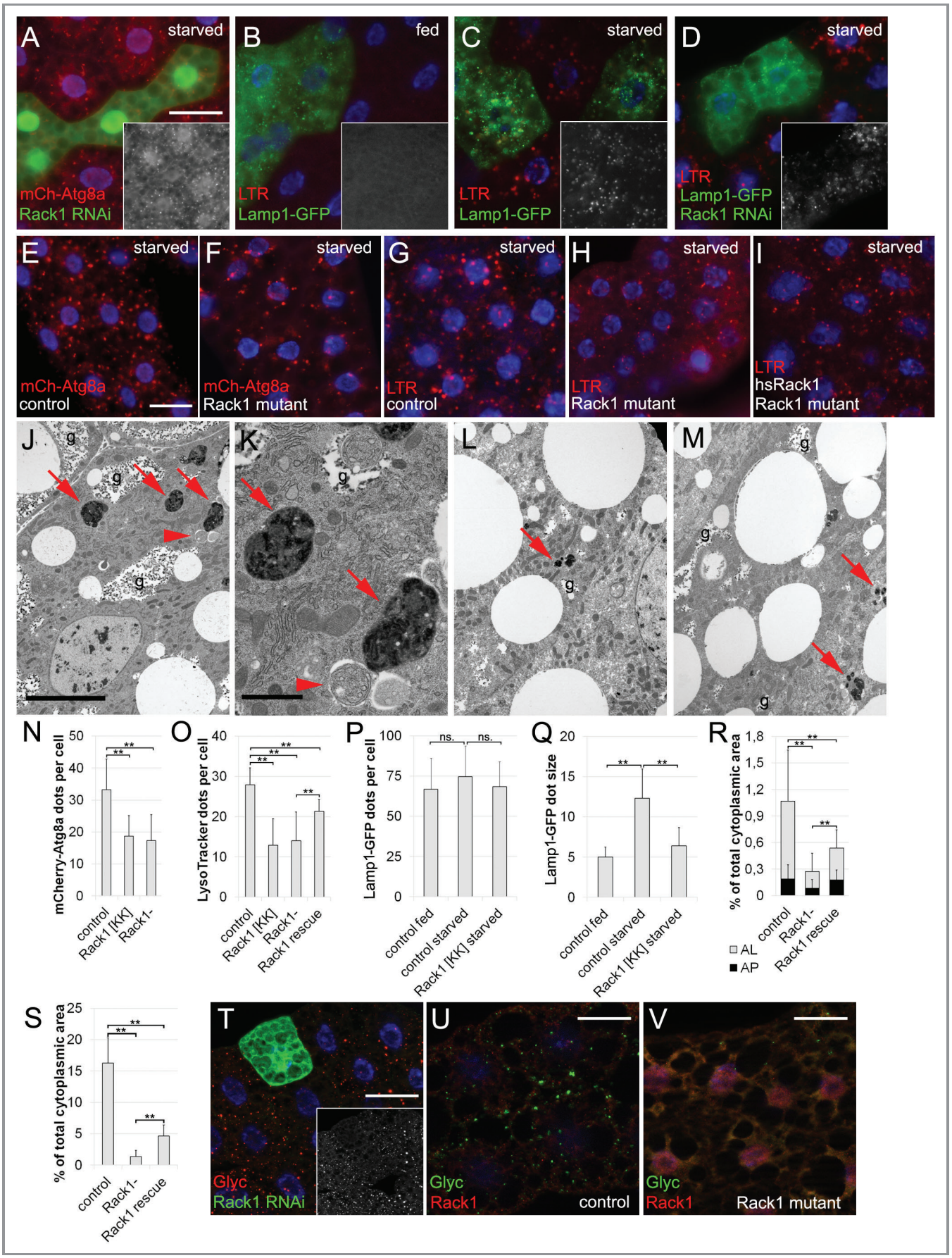

Immuno-electron microscopy analysis also identified that endogenous Rack1 localized in the periphery of, or immediately next to glycogen particles in fat body cells, in addition to being present in unidentified cytoplasmic clusters (**Fig. 3F and G**). In indirect immunofluorescence experiments most Rack1-positive dots localized next to or in the periphery of glycogen particles in laser scanning confocal microscopy as well (**Fig. 3H**). 77% of glycogen particles had associated Rack1 dots (n = 426/553), while 48% of Rack1 dots were associated with glycogen (n = 394/822).

The activity of glycogen synthase is a major determinant of glycogen levels. Phosphorylation of glycogen synthase by Shaggy, the Drosophila homolog of glycogen synthase kinase 3B (GSK-3B) promotes glycogen synthesis.[34] A physical interaction between the human homologs of Rack1 and GSK-3B was already reported.[35] In line with that, we found that 73.9% of endogenous Rack1 colocalized with endogenous Shaggy, and 39.4% of Shaggy positive dots were also positive for Rack1 (n = 82/111 and n = 82/208 dots, respectively) (**Fig. 3I**). In contrast, no colocalization was found between Shaggy and GFP-Atg8a (not shown).

Discussion

We have used whole-genome microarrays to identify genes regulated during the starvation response in Drosophila, and also compared gene expression changes between control, *Atg7* and *Atg1* mutant larvae. Based on a gene ontology analysis, genes involved in catabolic processes such as proteasomal degradation and amino acid catabolism were more significantly upregulated in starved autophagy mutants, which is likely a compensatory reaction. On the other hand, genes required for DNA replication were specifically downregulated. Mitotic tissues continue to grow and divide even in Drosophila larvae deprived of all nutrients.[36] Repression of genes required for DNA replication in autophagy mutants suggests that energy-consuming DNA replication processes are strongly inhibited in completely starved autophagy mutants, presumably because polyploid cells are not able to supply nutrients to support diploid cell divisions in the absence of autophagy.

We detected increased transcription of most *Atg* genes upon starvation, and an even higher upregulation was seen for most genes in fat bodies dissected from starved vs. fed animals. The most highly induced gene was *Atg8a* in all cases, in agreement with previous studies that showed the importance of *Atg8* induction during autophagy in various models.[1,12,15] It is important to note that *Atg8b* is mostly expressed in adult testis, and its very low level larval expression is restricted to the fat body.[37] In line with this, mutation of *Atg8a* completely blocks starvation-induced autophagy in the fat body confirming that *Atg8b* expression is unable to sustain autophagy in this setting, although *Atg8b* was also upregulated 118-fold during starvation in the fat body.[21] Induction of *Atg8a* is likely necessary to make up for the degradation of half of its protein products involved in each autophagosomal cycle. Members of the Atg9 cycling complex showed the strongest average upregulation of the functional groups of Atg proteins. We speculate that the sudden induction of autophagy in polyploid larval Drosophila tissues requires a lot of membrane to sustain the high level of autophagosome generation, explaining the increased transcription of genes whose products are required for membrane transport.

In this work we chose Rack1 (receptor of activated protein kinase C 1) for further analysis. *Rack1* was induced in whole animals and in dissected fat bodies during starvation, and loss of *Rack1* impaired both starvation-induced and basal autophagy, while it had no effect on developmentally programmed autophagy of the fat body. These findings indicate that Rack1 is involved in multiple but not all types of autophagy.

Autophagosomes generally have a short half-life of 5–10 min, which is the most likely explanation why basal levels of autophagy are very difficult to visualize in most tissues.[38] In contrast, autophagosomes appear in high numbers during starvation. The autophagosomal compartment was reduced in *Rack1* mutants which was rescued completely by transgenic expression of *Rack1*, and Rack1 was at least transiently associated with phagophore assembly sites and autophagosomes, altogether suggesting that Rack1 is required for efficient autophagosome formation. As we observed no defects in cell size/cell growth, DNA polyploidization or lipid droplet accumulation in *Rack1* loss of function cells, the autophagy defect seems to be a highly specific phenotype and not just a consequence of general problems with normal cellular functions.

Rack1 is an evolutionarily conserved guanine nucleotide-binding scaffold protein with a WD40-repeat: 77% (243/315) of the amino acid residues are identical and 87% (275/315) are similar between Drosophila Rack1 and human GNB2L1. A proteomic study of Atg complexes found that GNB2L1 interacts with human homologs of Atg1, Atg4, Atg14 and Atg18.[39] Although GNB2L1 was not classified as a high-confidence interacting partner, these data support our hypothesis that Rack1 may act as a scaffold, transiently binding multiple Atg proteins at phagophore assembly sites to promote maximal activity. In line with that, it is interesting to note that the potential interacting partners of human Rack1 include a member from all four Atg protein complexes. Further biochemical studies such as co-immunoprecipitation experiments are necessary to verify this hypothetical mechanism.

In addition, half of the Rack1-positive dots localized to glycogen particles, and loss of Rack1 prevented the proper formation of glycogen stores in larval fat body cells. The high degree of colocalization with GSK-3B strongly suggests that Rack1 is associated with a pool of GSK-3B that promotes glycogen synthesis. The known interacting partners of Rack1 include three subunits of AMPK (AMP-activated protein kinase): PRKAA1, PRKAA2 and PRKAB2. The β-subunit of AMPK has a glycogen-binding domain that targets a pool of this kinase to bind the surface of the glycogen particle. Activated AMPK turns on catabolic processes to generate ATP, and it also inhibits glycogen synthesis through direct phosphorylation of glycogen synthase.[40] We hypothesize that a signaling complex containing Rack1, GSK-3B and AMPK assembles on glycogen particles to regulate the rate of synthesis through phosphorylating different amino acid residues of glycogen synthase, with AMPK being responsible for targeting this complex to glycogen. In this scenario, the activity of

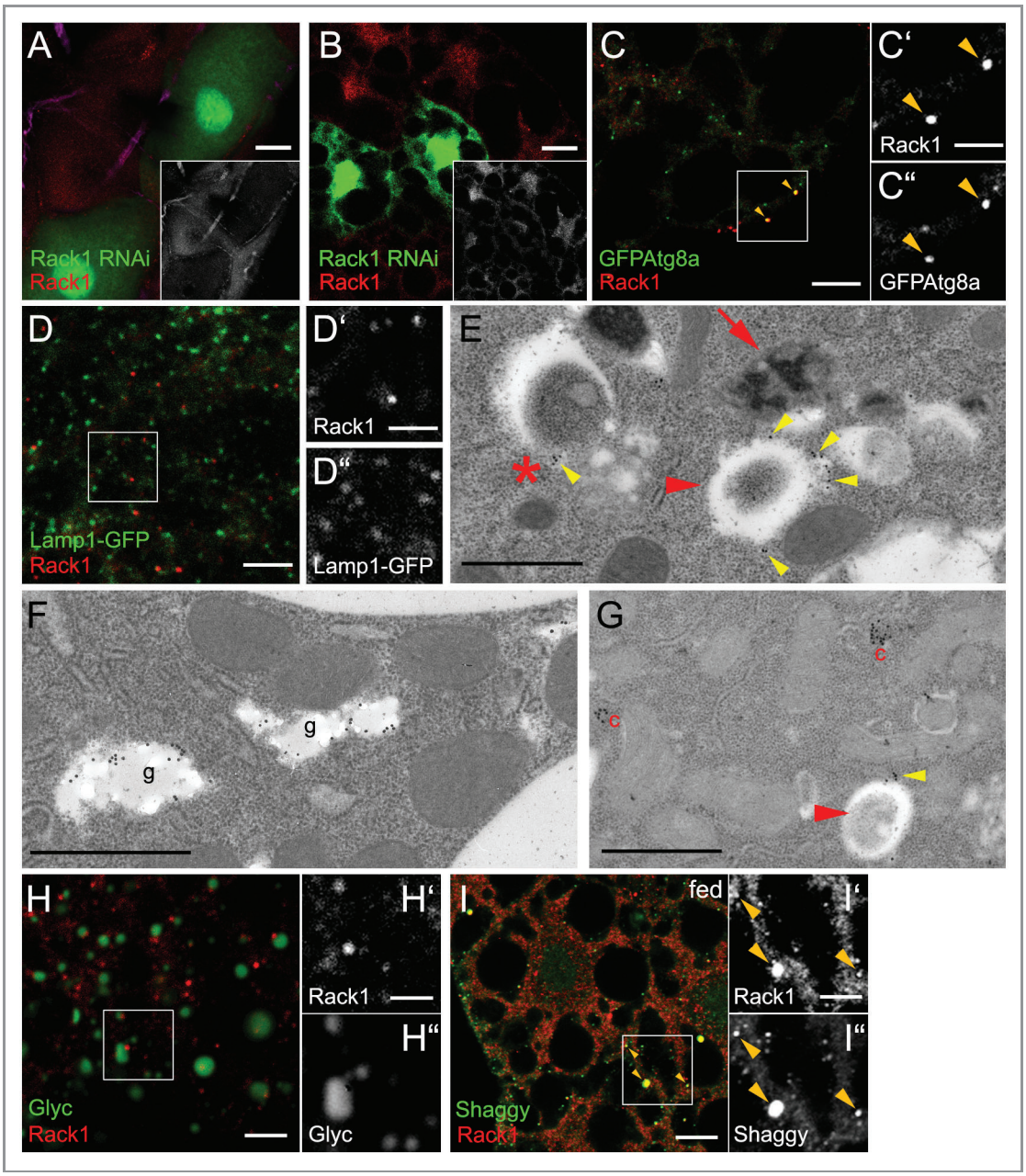

Figure 3. Localization of endogenous Rack1. (A and B) Knockdown of *Rack1* reduces anti-Rack1 immunostaining in both midgut and fat body cells in a cell-autonomous manner. (C) Rack1 shows a partial colocalization with the (pre-) autophagosome reporter GFP-Atg8a. (D) In contrast, no overlap was found between Rack1 and the lysosome reporter Lamp1-GFP. Boxed areas in (C and D) are shown enlarged. (E) Immunogold labeling of Rack1 is associated with a pre-autophagosomal phagophore near the growing edges (asterisk) and an autophagosome (red arrowhead). Please note the characteristic cleft (empty-looking space) between the two membrane sheets of phagophores and autophagosomes, which facilitates their recognition in glutaraldehyde-fixed samples. In contrast, no labeling of a lysosome is observed (arrow in E). Some of the gold particles are highlighted by yellow arrowheads. (F) Gold particles representing endogenous Rack1 are frequently associated with the peripheral parts of glycogen stores (g) in fat body cells. (G) Rack1 is also present in cytoplasmic clusters (c); an autophagosome (red arrowhead) is also labeled (yellow arrowhead). (H and I) Rack1 is closely associated with glycogen granules in the fat body, and it colocalizes with Shaggy, the Drosophila homolog of GSK-3B. Boxed areas of (A and B) are shown enlarged. Scale bars: 10 μm for (A–D, H and I), 5 μm for (C'–D" and H'–I") and 1 μm for (E–G). All colocalization experiments were performed using confocal laser scanning microscopy.

multiple kinases including AMPK and GSK-3B would determine the rate of glycogen synthesis. These interactions may be less relevant for Rack1's role in autophagy for a number of reasons. First, GSK-3B never colocalized with Atg8a, and overexpression of GSK-3B actually inhibits starvation-induced autophagy (our unpublished observation). Second, the exact role of AMPK in starvation-induced autophagy of the fat body is not clear: mutation of *SNF4Aγ* encoding a regulatory subunit of AMPK

has been shown to lead to impaired autophagic responses in mutants, but a more recent report suggested that AMPK mutants show a persistent starvation phenotype that may interfere with further induction of autophagy by additional experimental starvation.[41,42] In line with that, none of the more than 10 different transgenic RNAi and dominant-negative AMPK lines we tested showed any suppression of starvation-induced autophagy in clonal analysis (our unpublished observations), potentially supporting the hypothesis that the autophagy phenotype of AMPK mutants may not be cell autonomous in the Drosophila fat body.

Rack1 was originally described as a cytoplasmic receptor for activated protein kinase C (PKC). The structure of Rack1 resembles that of the β-subunit of heterotrimeric G proteins. The individual WD40 repeats can simultaneously bind to different proteins, making Rack1 a candidate platform for integrating several signaling pathways. Rack1 was shown to physically interact with β-integrin, various kinases including PKC, AMPK, GSK-3B and Src, protein phosphatase 2A, focal adhesion components, and even ribosomes. Indeed, Rack1 plays a role in a wide range of processes including cell adhesion and migration, cell survival and translation.[33,43] Recent findings showed that Rack1 promotes and is required for progression of several types of cancers, and its increased expression predicts poor clinical outcome for breast cancer patients.[44-48]

Here we have shown that Drosophila Rack1 is also involved in the autophagic response to starvation, potentially acting again as a scaffold protein during the formation of autophagosomes. In addition, Rack1 is necessary for the proper generation of glycogen particles in the larval fat body, likely through recruiting Shaggy/GSK-3B to promote glycogen synthesis. Taken together, we have demonstrated that novel roles in autophagy and glycogen synthesis must be added to the already diverse list of functions for Rack1.

Materials and Methods

Drosophila stocks and culture. Flies were raised at 25°C on standard cornmeal/agar media, at 60% humidity and a 12-h light/12-h dark daily cycle. The following stocks were used: *CG5335 [d30], Atg7[d77], Atg7[d14]*,[3] (d14 deletes the promoters and the first parts of both *Atg7* and *Sec6*, d77 deletes both *CG5335* and *Atg7,* and d30 deletes *CG5335* only; therefore, *d77/d14* animals are mutant for *Atg7* only and heterozygous for both *CG5335* and *Sec6*, while *d30/d14* are heterozygous for all three genes), *Atg1 [d3D]*,[21] *UAS-Lamp1-GFP, UAS-GFP-Atg8a*,[49] *hs-Flp; UAS-Dcr2; R4-mCherry-Atg8a, Act > CD2 > Gal4, UAS-GFPnls* (gift of Tom Neufeld), *Df(2L)rack1-mts, Rack1[1.8]*,[33] (the 1.8 allele carries a premature stop codon instead of the sixth amino acid; we used hemizygous animals in trans with the deficiency *Df(2L) rack1-mts* that deletes both *Rack1* and *mts* in all experiments), *hs-Gal4* (Bloomington Drosophila Stock Center, BDSC), and transgenic RNAi lines for *Rack1 KK104470* (designated as Rack1 RNAi throughout the text and figures), *HMS01173* (designated as Rack1 RNAi_2 in **Fig. S1F**) (provided by the Vienna Drosophila RNAi Center, VDRC and BDSC, respectively). Starvations were routinely performed by floating well-fed 72–96 h AEL (after egg laying) larvae on top of a 20% sucrose solution in an Eppendorf tube for 4 h. For complete starvations (no calorie), we placed well-fed animals onto filter papers soaked in PBS. Twenty to 30 larvae were transferred into a new vial amply supplemented with live yeast culture (high protein diet) 12–24 h before starvation to reduce crowding and make sure that all animals were well-fed at the onset of the starvation experiments, which is necessary for a proper autophagic response. For diet high in both protein and sugar, yeast paste was prepared in a 20% sucrose solution.

Microarray analysis. Our microarray experiments conformed to MIAME guidelines, and full data sets are available at www.ebi.ac.uk/arrayexpress under accession number E-MEXP-3352.

Four microarrays were used for analyzing each genotype: two independent fed and starved samples were collected (biological replica), and a dye swap was performed for each fed/starved sample pair (technical replica—please see below). Eighty-six ± 2 h AEL L3 stage larvae were allowed to feed on standard fly food supplemented with yeast (fed) or starved in PBS for 4 h (starved). Approximately 30 mg of larvae were collected and frozen immediately in liquid nitrogen in RNAlater (Sigma, R0901). Total RNA was purified using a NucleoSpin RNA II RNA isolation kit (Macherey-Nagel, 740955). RNA samples were stored at –80°C in the presence of 30 U Prime RNase inhibitor (Fermentas, EO0382). For probe preparation, 1 μg of total RNA were first reverse transcribed in 10 μl volume using Oligo(dT) Primer and ArrayScript enzyme, then the second cDNA strand was synthesized in 50 μl final volume using DNA polymerase and RNase H. Amino allyl modified aRNA were then synthesized by in vitro transcription using aaUTP and T7 Enzyme mix. All these steps were done using AminoAllyl MessageAmp™ II aRNA Amplification Kit (Ambion, AM1753). Six micrograms of amino allyl modified amplified RNA was labeled with either Cy5 or Cy3 dyes in 10 μl volume (GE Healthcare, PA23001, PA25001) and purified using RNA purification columns (Macherey Nagel, 740955). The specific activity and concentration of the labeled aRNA samples was checked by spectrophotometry (NanoDrop 3.1.0, Rockland). 4 × 44 k format Drosophila Gene Expression Microarrays (Agilent, G2519F-021791) were used to determine gene expression changes. 300 ng of Cy5 and Cy3 labeled aRNA in 19 μl volume, 5 μl 10 × blocking agent and 1 μl 25 × fragmentation buffer were mixed together and incubated at 60°C for 30 min. Twenty-five microliters 2× GEx hybridization fuffer was added to each sample to stop the fragmentation reaction. All these steps were done using gene expression hybridization kit (Agilent, 5188-5242). Forty-eight microliters of these mixes were used for the hybridization in microarray hybridization chambers (Agilent, G2534A). The chambers were then loaded into a hybridization rotator rack (~5 rpm) and incubated at 65°C for 17 h. After hybridization the slides were washed in wash buffer 1 (Agilent, 5188-5327) at room temperature for 1 min then in wash buffer 2 at 37°C for another 1 min before scanning. Each array was scanned at 543 nm (for Cy3 labeling) or at 633 nm (for Cy5 labeling) in Agilent Scanner using the built-in XDR (Extended Dynamic Range) function with 5 μm resolution. Output images were analyzed with the Feature

Extraction software from Agilent (ver.9.5.1.1.) using the two-color gene expression protocol (GE2_v5_95_Feb07) to get the raw data. All ratios were normalized using the Lowess normalization method. Two-tailed two-sample unequal variance Student's t-test with a two-fold change cut off was applied to determine which genes showed significantly altered expression levels ($p < 0.05$). Additionally, we applied multiple testing correction (Benjamini-Hochberg method; p value 2 in **Tables S1–S3**) using Genspring to estimate false discovery rate (corrected p value in supplemental tables) associated with such a large number of comparisons.

QT-PCR experiments. RNA samples were prepared from fat bodies dissected from fed and starved control larvae as described above. QT-PCR reactions were performed on 4 independently collected fed and 4 independently collected starved fat body samples. The reactions were performed on a RotorGene 3000 instrument (Corbett Research) with gene-specific primers and SybrGreen protocol to monitor gene expression. Two micrograms of total RNA was reverse transcribed using the High-Capacity cDNA Archive Kit (Applied Biosystems, 4322171) according to the manufacturer's instructions in a final volume of 30 μL. The temperature profile of the reverse transcription was the following: 10 min at room temperature, 2 h at 37°C, 5 min on ice and finally 10 min at 75°C for enzyme inactivation. After dilution with 30 μL of water, 1 μL of the diluted reaction mix was used as template in QT-PCR reactions, using FastStart SYBR Green Master mix (Roche, 04673484001) at a final primer concentration of 250 nM under the following conditions: 15 min at 95°C, 45 cycles of 95°C for 15 sec, 60°C for 25 sec and 72°C for 25 sec. Fluorescence intensity of SYBR Green was detected after each amplification step. Melting temperature analysis was done after each reaction to check the quality of the products. Relative expression ratios were calculated as normalized ratios to *GAPDH*. As an additional control, no significant change was observed in expression from the *Actin5C* locus. Nontemplate control sample was used for each PCR run to check the primer-dimer formation. The final relative gene expression ratios were calculated as ΔΔCt values. Primer sequences are available upon request. Two-tailed two-sample unequal variance Student's t-test was used to calculate p values.

Bioinformatic analysis. GO analysis was performed using DAVID Bioinformatics Resources 6.7 at http://david.niaid.nih.gov.[50] We selected unique FBgn identifiers of genes showing an at least two-fold expression change in response to starvation with $p < 0.05$ from all three genotypes. Separate lists of induced and repressed FBgn identifiers were uploaded, and the GO terms of biological processes functional annotation tool was used for functional annotation clustering with default options. We then compared the significantly enriched ($p < 0.05$) GO categories among the three genotypes. As most genes are represented by multiple 60-mer oligos on the whole-genome microarray, all $p < 0.05$ fold change values were collected for each gene of interest, averaged, and then visualized using JColorGrid for the expression analysis of individual *Atg* genes.[51] BLASTP searches were used to find homologous gene products in yeast, Drosophila and human, and the top-scoring hit is shown for each gene in **Figure 1C**.

Construction of UAS-Rack1 transgenic lines and genetic rescue experiments. The pUAST-Rack1-FLAG-HA clone UFO04269 was obtained from DGRC (Drosophila Genomics Resource Center). Following sequencing, standard PhiC31-mediated transformation procedures were used to obtain transgenic Drosophila lines carrying *UAS-Rack1* on a 65B2 platform chromosome (Bestgene). Expression of *UAS-Rack1* was induced with hs-Gal4 in a *Rack1* null mutant background by a 1 h heat shock at 37°C, followed by a 4 h starvation.

Histology and imaging. Clonal analysis in polyploid larval Drosophila tissues and Lysotracker stainings were performed as described previously.[21,49] For statistics, Lysotracker, mCherry-Atg8a and Lamp1-GFP puncta were manually counted in Photoshop. Two-tailed two-sample unequal variance Student's t-test was used to calculate p values. The following antibodies were used for immunostainings: rabbit polyclonal anti-Rack1 (1:500, gift from Julie Kadrmas),[33] mouse monoclonal anti-glycogen (1:20, gift from Otto Baba),[52] mouse monoclonal anti-Shaggy (4G1E11, 1:100, gift from Marc Bourouis),[34] mouse monoclonal anti-GFP (1:1,000, Invitrogen, A11120), Alexa488-conjugated goat anti-mouse (Invitrogen, A11001, 1:1,000), Alexa568-conjugated goat anti-rabbit (Invitrogen, A21069, 1:1,000). A Zeiss Axioimager M2 microscope equipped with an Apotome2 unit and a Plan-NeoFluar 40× 0.75 NA objective was used to capture images with Axiovision software using MinMax setting for automatically adjusting image levels. Confocal images were acquired on an Olympus FV500 laser scanning microscope with a 63× 1.45 NA oil-immersion objective in sequential scanning mode. Primary images were processed in Adobe Photoshop to produce final figures.

Transmission electron microscopy (TEM). Tissues were processed for TEM analysis as described previously.[49] For immuno-electron microscopy, rabbit polyclonal anti-Rack1 (1:50) was used as described previously.[3] Images were captured on a JEOL JEM-1011 transmission electron microscope using an Olympus Morada 11 megapixel camera and iTEM software (Olympus). For statistical analysis, four 5,000 × magnification images were taken randomly from four larvae in each genotype (16 images per genotype), and the area of autophagic structures and glycogen has been manually encircled in Photoshop to obtain area values. Relative cytoplasmic area values and two-tailed two-sample unequal variance Student's t-tests were calculated using Excel.

Disclosure of Potential Conflicts of Interest

No potential conflicts of interest were disclosed.

Acknowledgments

We thank Sarolta Pálfia for her excellent technical assistance, Otto Baba, Marc Bourouis and Julie Kadrmas for providing antibodies, Tom Neufeld and stock centers BDSC and VDRC for fly strains. This work was supported by the Wellcome Trust (087518/Z/08/Z), the Hungarian Scientific Research Fund (OTKA PD72095), the Hungarian Academy of Sciences (BO/00712/07, BO/00781/11, BO/00552/11) and the European Union and the European Social Fund contributed to the purchase of the electron microscope (TÁMOP 4.2.1./B-09/1/KMR-2010-0003).

Supplemental Materials

Supplemental materials may be found here:
www.landesbioscience.com/journals/autophagy/article/20069

References

1. Klionsky DJ, Emr SD. Autophagy as a regulated pathway of cellular degradation. Science 2000; 290:1717-21; PMID:11099404; http://dx.doi.org/10.1126/science.290.5497.1717
2. Hara T, Nakamura K, Matsui M, Yamamoto A, Nakahara Y, Suzuki-Migishima R, et al. Suppression of basal autophagy in neural cells causes neurodegenerative disease in mice. Nature 2006; 441:885-9; PMID:16625204; http://dx.doi.org/10.1038/nature04724
3. Juhász G, Erdi B, Sass M, Neufeld TP. Atg7-dependent autophagy promotes neuronal health, stress tolerance, and longevity but is dispensable for metamorphosis in Drosophila. Genes Dev 2007; 21:3061-6; PMID:18056421; http://dx.doi.org/10.1101/gad.1600707
4. Komatsu M, Waguri S, Chiba T, Murata S, Iwata J, Tanida I, et al. Loss of autophagy in the central nervous system causes neurodegeneration in mice. Nature 2006; 441:880-4; PMID:16625205; http://dx.doi.org/10.1038/nature04723
5. Simonsen A, Cumming RC, Brech A, Isakson P, Schubert DR, Finley KD. Promoting basal levels of autophagy in the nervous system enhances longevity and oxidant resistance in adult Drosophila. Autophagy 2008; 4:176-84; PMID:18059160
6. Klionsky DJ, Cregg JM, Dunn WA, Jr., Emr SD, Sakai Y, Sandoval IV, et al. A unified nomenclature for yeast autophagy-related genes. Dev Cell 2003; 5:539-45; PMID:14536056; http://dx.doi.org/10.1016/S1534-5807(03)00296-X
7. Hosokawa N, Hara T, Kaizuka T, Kishi C, Takamura A, Miura Y, et al. Nutrient-dependent mTORC1 association with the ULK1-Atg13-FIP200 complex required for autophagy. Mol Biol Cell 2009; 20:1981-91; PMID:19211835; http://dx.doi.org/10.1091/mbc.E08-12-1248
8. Nakatogawa H, Ishii J, Asai E, Ohsumi Y. Atg4 recycles inappropriately lipidated Atg8 to promote autophagosome biogenesis. Autophagy 2012; 8:177-86; PMID:22240591; http://dx.doi.org/10.4161/auto.8.2.18373
9. Tanida I, Sou YS, Ezaki J, Minematsu-Ikeguchi N, Ueno T, Kominami E. HsAtg4B/HsApg4B/autophagin-1 cleaves the carboxyl termini of three human Atg8 homologues and delipidates microtubule-associated protein light chain 3- and GABAA receptor-associated protein-phospholipid conjugates. J Biol Chem 2004; 279:36268-76; PMID:15187094; http://dx.doi.org/10.1074/jbc.M401461200
10. Orsi A, Polson HE, Tooze SA. Membrane trafficking events that partake in autophagy. Curr Opin Cell Biol 2010; 22:150-6; PMID:20036114; http://dx.doi.org/10.1016/j.ceb.2009.11.013
11. Mammucari C, Milan G, Romanello V, Masiero E, Rudolf R, Del Piccolo P, et al. FoxO3 controls autophagy in skeletal muscle in vivo. Cell Metab 2007; 6:458-71; PMID:18054315; http://dx.doi.org/10.1016/j.cmet.2007.11.001
12. Sandri M. Autophagy in skeletal muscle. FEBS Lett 2010; 584:1411-6; PMID:20132819; http://dx.doi.org/10.1016/j.febslet.2010.01.056
13. Lee CY, Clough EA, Yellon P, Teslovich TM, Stephan DA, Baehrecke EH. Genome-wide analyses of steroid- and radiation-triggered programmed cell death in Drosophila. Curr Biol 2003; 13:350-7; PMID:12593803; http://dx.doi.org/10.1016/S0960-9822(03)00085-X
14. Gorski SM, Chittaranjan S, Pleasance ED, Freeman JD, Anderson CL, Varhol RJ, et al. A SAGE approach to discovery of genes involved in autophagic cell death. Curr Biol 2003; 13:358-63; PMID:12593804; http://dx.doi.org/10.1016/S0960-9822(03)00082-4
15. Juhász G, Puskás LG, Komonyi O, Erdi B, Maróy P, Neufeld TP, et al. Gene expression profiling identifies FKBP39 as an inhibitor of autophagy in larval Drosophila fat body. Cell Death Differ 2007; 14:1181-90; PMID:17363962; http://dx.doi.org/10.1038/sj.cdd.4402123
16. Weidberg H, Shpilka T, Shvets E, Abada A, Shimron F, Elazar Z. LC3 and GATE-16 N termini mediate membrane fusion processes required for autophagosome biogenesis. Dev Cell 2011; 20:444-54; PMID:21497758; http://dx.doi.org/10.1016/j.devcel.2011.02.006
17. Rusten TE, Lindmo K, Juhász G, Sass M, Seglen PO, Brech A, et al. Programmed autophagy in the Drosophila fat body is induced by ecdysone through regulation of the PI3K pathway. Dev Cell 2004; 7:179-92; PMID:15296715; http://dx.doi.org/10.1016/j.devcel.2004.07.005
18. Scott RC, Schuldiner O, Neufeld TP. Role and regulation of starvation-induced autophagy in the Drosophila fat body. Dev Cell 2004; 7:167-78; PMID:15296714; http://dx.doi.org/10.1016/j.devcel.2004.07.009
19. Zinke I, Schütz CS, Katzenberger JD, Bauer M, Pankratz MJ. Nutrient control of gene expression in Drosophila: microarray analysis of starvation and sugar-dependent response. EMBO J 2002; 21:6162-73; PMID:12426388; http://dx.doi.org/10.1093/emboj/cdf600
20. Beadle G, Tatum EL, Clancy CW. Food level in relation to rate of development and eye pigmentation in Drosophila melanogaster. Biol Bull 1938; 75:447-62; http://dx.doi.org/10.2307/1537573
21. Scott RC, Juhász G, Neufeld TP. Direct induction of autophagy by Atg1 inhibits cell growth and induces apoptotic cell death. Curr Biol 2007; 17:1-11; PMID:17208179; http://dx.doi.org/10.1016/j.cub.2006.10.053
22. Tweedie S, Ashburner M, Falls K, Leyland P, McQuilton P, Marygold S, et al. FlyBase Consortium. FlyBase: enhancing Drosophila Gene Ontology annotations. Nucleic Acids Res 2009; 37 (Database issue):D555-9; PMID:18948289; http://dx.doi.org/10.1093/nar/gkn788
23. Becker T, Loch G, Beyer M, Zinke I, Aschenbrenner AC, Carrera P, et al. FOXO-dependent regulation of innate immune homeostasis. Nature 2010; 463:369-73; PMID:20090753; http://dx.doi.org/10.1038/nature08698
24. Bülow MH, Aebersold R, Pankratz MJ, Jünger MA. The Drosophila FoxA ortholog Fork head regulates growth and gene expression downstream of Target of rapamycin. PLoS One 2010; 5:e15171; PMID:21217822; http://dx.doi.org/10.1371/journal.pone.0015171
25. Yauk CL, Berndt ML, Williams A, Douglas GR. Comprehensive comparison of six microarray technologies. Nucleic Acids Res 2004; 32:e124; PMID:15333675; http://dx.doi.org/10.1093/nar/gnh123
26. Hosokawa N, Sasaki T, Iemura S, Natsume T, Hara T, Mizushima N. Atg101, a novel mammalian autophagy protein interacting with Atg13. Autophagy 2009; 5:973-9; PMID:19597335; http://dx.doi.org/10.4161/auto.5.7.9296
27. Mercer CA, Kaliappan A, Dennis PB. A novel, human Atg13 binding protein, Atg101, interacts with ULK1 and is essential for macroautophagy. Autophagy 2009; 5:649-62; PMID:19287211; http://dx.doi.org/10.4161/auto.5.5.8249
28. Vergne I, Roberts E, Elmaoued RA, Tosch V, Delgado MA, Proikas-Cezanne T, et al. Control of autophagy initiation by phosphoinositide 3-phosphatase Jumpy. EMBO J 2009; 28:2244-58; PMID:19590496; http://dx.doi.org/10.1038/emboj.2009.159
29. Mari M, Griffith J, Rieter E, Krishnappa L, Klionsky DJ, Reggiori F. An Atg9-containing compartment that functions in the early steps of autophagosome biogenesis. J Cell Biol 2010; 190:1005-22; PMID:20855505; http://dx.doi.org/10.1083/jcb.200912089
30. Pankiv S, Clausen TH, Lamark T, Brech A, Bruun JA, Outzen H, et al. p62/SQSTM1 binds directly to Atg8/LC3 to facilitate degradation of ubiquitinated protein aggregates by autophagy. J Biol Chem 2007; 282:24131-45; PMID:17580304; http://dx.doi.org/10.1074/jbc.M702824200
31. Simonsen A, Birkeland HC, Gillooly DJ, Mizushima N, Kuma A, Yoshimori T, et al. Alfy, a novel FYVE-domain-containing protein associated with protein granules and autophagic membranes. J Cell Sci 2004; 117:4239-51; PMID:15292400; http://dx.doi.org/10.1242/jcs.01287
32. Pulipparacharuvil S, Akbar MA, Ray S, Sevrioukov EA, Haberman AS, Rohrer J, et al. Drosophila Vps16A is required for trafficking to lysosomes and biogenesis of pigment granules. J Cell Sci 2005; 118:3663-73; PMID:16046475; http://dx.doi.org/10.1242/jcs.02502
33. Kadrmas JL, Smith MA, Pronovost SM, Beckerle MC. Characterization of RACK1 function in Drosophila development. Dev Dyn 2007; 236:2207-15; PMID:17584887; http://dx.doi.org/10.1002/dvdy.21217
34. Papadopoulou D, Bianchi MW, Bourouis M. Functional studies of shaggy/glycogen synthase kinase 3 phosphorylation sites in Drosophila melanogaster. Mol Cell Biol 2004; 24:4909-19; PMID:15143183; http://dx.doi.org/10.1128/MCB.24.11.4909-4919.2004
35. De Toni-Costes F, Despeaux M, Bertrand J, Bourogaa E, Ysebaert L, Payrastre B, et al. A New alpha5beta1 integrin-dependent survival pathway through GSK3beta activation in leukemic cells. PLoS One 2010; 5:e9807; PMID:20352103; http://dx.doi.org/10.1371/journal.pone.0009807
36. Britton JS, Edgar BA. Environmental control of the cell cycle in Drosophila: nutrition activates mitotic and endoreplicative cells by distinct mechanisms. Development 1998; 125:2149-58; PMID:9570778
37. Chintapalli VR, Wang J, Dow JA. Using FlyAtlas to identify better Drosophila melanogaster models of human disease. Nat Genet 2007; 39:715-20; PMID:17534367; http://dx.doi.org/10.1038/ng2049

38. Mizushima N, Yamamoto A, Matsui M, Yoshimori T, Ohsumi Y. In vivo analysis of autophagy in response to nutrient starvation using transgenic mice expressing a fluorescent autophagosome marker. Mol Biol Cell 2004; 15:1101-11; PMID:14699058; http://dx.doi.org/10.1091/mbc.E03-09-0704
39. Behrends C, Sowa ME, Gygi SP, Harper JW. Network organization of the human autophagy system. Nature 2010; 466:68-76; PMID:20562859; http://dx.doi.org/10.1038/nature09204
40. Hardie DG. Energy sensing by the AMP-activated protein kinase and its effects on muscle metabolism. Proc Nutr Soc 2011; 70:92-9; PMID:21067629; http://dx.doi.org/10.1017/S0029665110003915
41. Johnson EC, Kazgan N, Bretz CA, Forsberg LJ, Hector CE, Worthen RJ, et al. Altered metabolism and persistent starvation behaviors caused by reduced AMPK function in Drosophila. PLoS One 2010; 5:5; PMID:20862213; http://dx.doi.org/10.1371/journal.pone.0012799
42. Lippai M, Csikós G, Maróy P, Lukácsovich T, Juhász G, Sass M. SNF4Agamma, the Drosophila AMPK gamma subunit is required for regulation of developmental and stress-induced autophagy. Autophagy 2008; 4:476-86; PMID:18285699
43. Nilsson J, Sengupta J, Frank J, Nissen P. Regulation of eukaryotic translation by the RACK1 protein: a platform for signalling molecules on the ribosome. EMBO Rep 2004; 5:1137-41; PMID:15577927; http://dx.doi.org/10.1038/sj.embor.7400291
44. Bertrand J, Despeaux M, Joly S, Bourogaa E, Gallay N, Demur C, et al. Sex differences in the GSK3beta-mediated survival of adherent leukemic progenitors. Oncogene 2011; 31:694-705; PMID:21725365; http://dx.doi.org/10.1038/onc.2011.258
45. Wang F, Osawa T, Tsuchida R, Yuasa Y, Shibuya M. Down-regulation of RACK1 suppresses tumor growth by inhibiting tumor cell proliferation and tumor-associated angiogenesis. Cancer Sci 2011; 102:2007-13; PMID:21848913; http://dx.doi.org/10.1111/j.1349-7006.2011.02065.x
46. Cao XX, Xu JD, Liu XL, Xu JW, Wang WJ, Li QQ, et al. RACK1: A superior independent predictor for poor clinical outcome in breast cancer. Int J Cancer 2010; 127:1172-9; PMID:20020495; http://dx.doi.org/10.1002/ijc.25120
47. Cao XX, Xu JD, Xu JW, Liu XL, Cheng YY, Wang WJ, et al. RACK1 promotes breast carcinoma proliferation and invasion/metastasis in vitro and in vivo. Breast Cancer Res Treat 2010; 123:375-86; PMID:19946739; http://dx.doi.org/10.1007/s10549-009-0657-x
48. Nagashio R, Sato Y, Matsumoto T, Kageyama T, Satoh Y, Shinichiro R, et al. Expression of RACK1 is a novel biomarker in pulmonary adenocarcinomas. Lung Cancer 2010; 69:54-9; PMID:19892429; http://dx.doi.org/10.1016/j.lungcan.2009.09.015
49. Juhász G, Hill JH, Yan Y, Sass M, Baehrecke EH, Backer JM, et al. The class III PI(3)K Vps34 promotes autophagy and endocytosis but not TOR signaling in Drosophila. J Cell Biol 2008; 181:655-66; PMID:18474623; http://dx.doi.org/10.1083/jcb.200712051
50. Huang W, Sherman BT, Lempicki RA. Systematic and integrative analysis of large gene lists using DAVID bioinformatics resources. Nat Protoc 2009; 4:44-57; PMID:19131956; http://dx.doi.org/10.1038/nprot.2008.211
51. Joachimiak MP, Weisman JL, May BCh. JColorGrid: software for the visualization of biological measurements. BMC Bioinformatics 2006; 7:225; PMID:16640789; http://dx.doi.org/10.1186/1471-2105-7-225
52. Baba O. Production of monoclonal antibody that recognizes glycogen and its application for immunohistochemistry. Kokubyo Gakkai Zasshi 1993; 60:264-87; PMID:8345245; http://dx.doi.org/10.5357/koubyou.60.264